STRUCTURE OF THE ^{115}Ag EXCITED STATES FROM IBFM-1 CALCULATIONS

S. Kisyov

Lawrence Berkeley National Laboratory, Berkeley, CA 94720, USA

S. Lalkovski

Faculty of Physics, Sofia University "St. Kliment Ohridski", Sofia 1164, Bulgaria

Received 8 October 2024, accepted 11 December 2024, published online 18 December 2024

The structure of the neutron mid-shell $^{115}_{47}Ag_{68}$ nucleus was analyzed via Interacting Boson–Fermion Model (IBFM) calculations. Excited level energies and electromagnetic properties of ^{115}Ag were calculated by using a proton hole coupled to an even–even ^{116}Cd core described within the extended consistent Q formalism (ECQF). The new theoretical results are in a good agreement with the available experimental data and show a dominant $\pi g_{9/2}$ component in the wave functions of the low-energy positive-parity states. The calculations provide insight into the ordering of the $7/2^+_1$ and $9/2^+_1$ states and the known $j-1$ anomaly along the silver isotopic chain.

DOI:10.5506/APhysPolB.55.11-A4

1. Introduction

A vast amount of new experimental data for neutron-rich nuclei from the $A \sim 110$ region has been acquired due to recent advances in the γ-ray detection technologies [1–4] and radioactive beam facilities [5–9]. This nuclear mass region exhibits very complex characteristics, some of which can be identified within a broader overview of several isotopic chains. The structure can dramatically change with the addition or subtraction of just a few particles, as it is well known from Zr nuclei [10, 11]. In addition, octupole deformation emerges in the Zr [12] and Mo [13] isotopic chains near $N = 56$. Effects of triaxiality manifest in Tc [14, 15], Ru [16–18], Rh [19], and Pd [20–23] nuclei, while the neutron mid-shell Cd isotopes are textbook examples for quadrupole vibrations [24, 25]. All these observations emphasize the diversity and richness of phenomena in the $A \sim 110$ mass region and characterize an extensive landscape of numerous structural effects.

While not necessarily exhibiting each of the aforementioned phenomena, silver nuclei in this mass region show some particular characteristics which challenge model interpretations. The yrast excitations of the semi-magic ^{97}Ag nucleus can be well explained by single-j three-hole configurations. Quadrupole deformation develops with an increase in the neutron number along the Ag isotopic chain [26]. One of the striking features of the Ag isotopes is the so-called "$j-1$ anomaly". The effect is related to the re-ordering of the $(j,\, j-1)$ states of the single-j j^{-3} multiplet. According to the nuclear shell model [27], the j state is the lowest energy state. In Ag, structures similar to the j^{-3} arise and are associated with the $\pi g_{9/2}^{-3}$ configuration. It is instructive to note that within the $\pi g_{9/2}^{-3}$ approach, the energy spectrum consists of states with angular momenta from $3/2^+$ to $21/2^+$, except for $19/2^+$ which is not a part of the multiplet. All these states have a seniority number $\upsilon = 3$, except for the $9/2^+$ level which has $\upsilon = 1$. However, simplified shell model calculations with three valence holes could not reproduce well the transition rates between the $I = j$ and $I = j - 1$ members of the multiplet [28].

The presence of $7/2_1^+$ states with excitation energy lower than the ones of the $9/2_1^+$ levels is observed along all Ag isotopes between ^{103}Ag and ^{123}Ag [29]. This effect was investigated via different theoretical approaches over the years. Such are studies performed considering breaking the jj-coupling approximation and introducing $g_{7/2}^n$ admixtures to the wave functions [30], the j^{-3} coupling scheme [31], shell model calculations with effective $Q\,Q$ and surface delta (SDI) interactions [32, 33], three-valence holes-vibrator coupling model calculations [28], IBFM [34], *etc.* While such anomalous behavior is also observed in other isotopic and isotonic chains [26, 32, 35], it is very prominent in the medium-mass and heavy silver nuclei [26]. Recent systematic works [26, 34, 36–38] show that the $j,\, j-1$ energy gap is strongly correlated with the energies of the 2^+ states in neighboring even-A nuclei. It could be, therefore, expected that core excitations play an important role in the development of the low-energy part of the Ag spectrum.

Generally, the positive-parity bands observed in the heavier silver isotopes do not resemble the weak particle–core coupling scheme of Ref. [39]. The neutron mid-shell Ag nuclei rather show fingerprints of a deformed odd-mass system [40]. Yet, there are features which cannot be understood within the particle–rotor approach. The positive-parity sequences in several Ag isotopes terminate at $J^\pi = 21/2^+$ which is typical for the $\pi g_{9/2}^{-3}$ scheme [29]. A similar band-termination mechanism is found in the IBFM-1 model with O(6) symmetry of the bosonic system [41], where the maximum spin of the band is limited by the number of bosons. However, mid-shell Ag isotopes have far fewer valence particles for a termination of the positive-parity band at $21/2^+$ to occur.

Despite the large variety of theoretical investigations, the structure of the silver nuclei still remains elusive. This is problematic not only in the microscopic world of nuclear structure but it can also have consequences for some larger-scale processes. For example, low-lying isomeric states in $^{111-115}$Ag (such as the $7/2_1^+$ state in ^{115}Ag having a half-life $T_{1/2} = 18.0$ (7) s) impact the nucleosynthesis mechanisms contributing to the astrophysical origin and abundance of rare isotopes in the Cd–In–Sn region [42, 43]. Therefore, detailed knowledge about the structure of the Ag nuclei can be also essential in astrophysics and, in particular, due to the implications to the isotope abundance calculations.

The present work focuses on a theoretical description of the structure of ^{115}Ag within IBFM-1 [44]. IBFM calculations have been previously performed to study silver nuclei but they either mainly focus on intruder states [45], or investigate lower-mass odd-A Ag isotopes [46–50]. The current calculations provide a complete set of information about level schemes and electromagnetic properties in ^{115}Ag. The present work extends the approach we used for the description of $^{111-113}$Ag [34], therefore providing a broader systematic study of the Ag mid-shell nuclei within IBFM-1. The collective properties of both ^{115}Ag and its even–even core are discussed in the context of developed quadrupole deformation.

2. IBFM calculations

Earlier IBFM works on odd-A Ag isotopes provide various arguments in favor of using either of both possible coupling schemes — coupling of a proton to a Pd even–even core, or a proton hole coupled to a Cd core [45–50]. The choices made were mostly motivated by the amount of available experimental data, the presence of intruder states, and a degree of collectivity in the core nucleus. In the frame of IBM, the Cd isotopes have the structure closer to the U(5) limit, while Pd nuclei exhibit a more transitional O(6) character. In our systematic study, including ^{111,113}Ag [34] and the present work, we observed a generally better description of the mid-shell odd-A Ag energy level schemes using the proton hole–Cd coupling.

2.1. IBM-1 calculations of ^{116}Cd

The properties of ^{116}Cd were calculated by using the extended consistent-Q formalism (ECQF) to IBM-1. This theoretical approach was introduced to allow for description of a complex set of collective structure effects, spanning over from vibrational through rotational to γ-unstable nuclei [51, 52]. The ECQF Hamiltonian is

$$H = \varepsilon n_d - \kappa Q^2 - \kappa' L^2 \,. \tag{1}$$

with

$$\begin{aligned} n_d &= \sqrt{5}\, T_0\,, \\ L &= \sqrt{10}\, T_1\,, \\ Q &= \left(d^\dagger s + s^\dagger \tilde{d}\right) + \chi \left(d^\dagger \tilde{d}\right)^{(2)} = \left(d^\dagger s + s^\dagger \tilde{d}\right) + \chi T_2\,, \\ \tilde{d}_\mu &= (-1)^\mu d_{-\mu}\,. \end{aligned} \tag{2}$$

The IBM-1 calculations were performed by using the PHINT program package [53]. The model parameters presented in Table 1 were obtained after a fit to the experimental data for ^{116}Cd. This set of parameters describes well the excitation energies of the low-lying states in ^{116}Cd (see Fig. 1), as well as the E2 transition strengths. It is consistent with earlier similar approaches applied to ^{112,114}Cd [34]. The parameters used in these studies are, in general, similar to the ones used in an ECQF IBM-1 description of even–even Ru and Pd isotopes [52, 54].

Table 1. IBM-1 set of parameters used to calculate the properties of the ^{116}Cd core.

ε	κ	κ'	χ	e_B
0.69	0.0208	−0.0045	−0.411	0.095

An E2 transitions operator in the form

$$T(\mathrm{E2}) = e_B \left[\left(s^\dagger \tilde{d} + d^\dagger s\right) + \chi \left(d^\dagger \tilde{d}\right)^{(2)} \right] = e_B Q \tag{3}$$

was used to calculate transition probabilities, with

$$B(\mathrm{E2}; J_\mathrm{i} \to J_\mathrm{f}) = \frac{1}{2J_\mathrm{i}+1} \left\langle J_\mathrm{f} \| T(\mathrm{E2}) \| J_i \right\rangle^2 , \tag{4}$$

where J_i and J_f denote the spins of the initial and final states, respectively.

A comparison between calculated and experimental $B(\mathrm{E2})$ values of several low-lying transitions in ^{116}Cd is presented in Table 2. A good agreement between the theoretical values and experimental data is achieved. The electromagnetic properties of ^{116}Cd were further investigated within IBM-1 by calculating the quadrupole moments (Q) of the first excited 2^+ and 4^+ states. The IBM-1 $Q_\mathrm{th}(2^+) = -0.28$ eb is consistent with the evaluated experimental result of $Q_\mathrm{exp}(2^+) = -0.42$ (4) b [55]. Furthermore, the calculations also suggest $Q_\mathrm{th}(4^+) = -0.41$ eb.

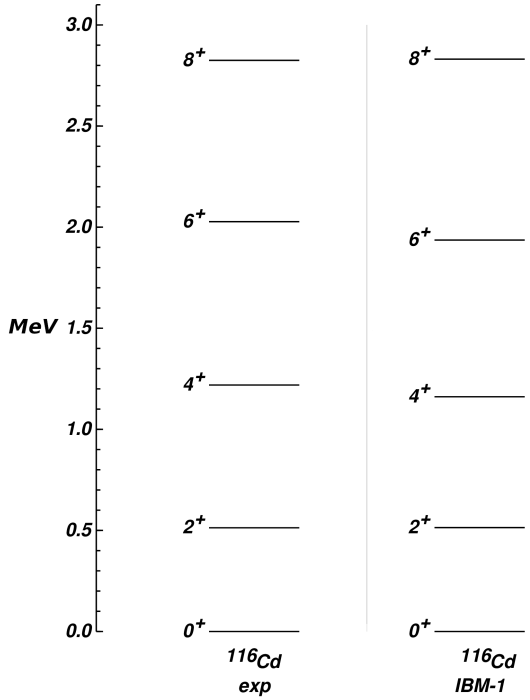

Fig. 1. A comparison between experimental and IBM-1 calculated levels in ^{116}Cd. The experimental data are taken from Ref. [55].

Table 2. Experimental and IBM-1 calculated B(E2) values for transitions between low-lying states in ^{116}Cd. The experimental data are taken from Ref. [55].

J_i^π	E_γ [keV]	J_f^π	$B(\mathrm{E2})_{\mathrm{exp}}$ [W.u.]	$B(\mathrm{E2})_{\mathrm{th}}$ [W.u.]
2^+	513.49	0^+	33.5 (12)	33.7
4^+	705.96	2^+	56 (14)	53
6^+	807.21	4^+	110 (80)	63
8^+	798.24	6^+		66

The quadrupole moments data provide essential information about the structure of ^{116}Cd. Neighboring even–even Ru and Pd isotopes in this mass region indicate a transition between the U(5) and O(6) limits of IBM [54, 56], while the Cd isotopes are often given as an example of vibrational-like nuclei. The non-zero theoretical and experimental quadrupole moments in ^{116}Cd suggest certain deviations from the O(6) limit of IBM (which is characterized

by vanishing Q), as well as from the pure U(5) behavior. A non-zero value of the χ parameter was used in the present IBM-1 approach and while being close to the U(5) limit, deviations from its paradigm were introduced.

2.2. IBFM-1 approach to ^{115}Ag

The IBFM-1 calculations to reproduce the properties of ^{115}Ag were performed by using the ^{116}Cd IBM-1 core and a Hamiltonian in the form

$$H = H_B + H_F + V_{BF}\,, \tag{5}$$

where H_B denotes the ^{116}Cd IBM-1 Hamiltonian and the fermionic term is

$$H_F = \sum_j E_j n_j\,. \tag{6}$$

E_j denotes the quasiparticle energies of the single-particle shell model orbitals.

The boson–fermion interaction V_{BF} is described by several interactions, which are sufficient for a phenomenological study of the different properties [57, 58]

$$\begin{aligned} V_{BF} \;=\; & \sum_j A_j n_d n_j + \sum_{jj'} \Gamma_{jj'} \left(Q \left(a_j^\dagger \tilde{a}_{j'} \right)^{(2)} \right) \\ & + \sum_{jj'j''} \Lambda_{jj'}^{j''} : \left(\left(d^\dagger \tilde{a}_j \right)^{(j'')} \left(\tilde{d} a_{j'}^\dagger \right)^{(j'')} \right)_0^{(0)} : \,. \end{aligned} \tag{7}$$

Based on microscopic considerations, the number of parameters can be decreased, leading to [59]

$$\begin{aligned} A_j &= A_0\,, \\ \Gamma_{jj'} &= \Gamma_0 \left(u_j u_{j'} - v_j v_{j'} \right) \left\langle j \left\| Y^{(2)} \right\| j' \right\rangle\,, \\ \Lambda_{jj'}^{j''} &= -2\sqrt{5}\Lambda_0 \beta_{jj''}\beta_{j''j'} / \left(2j''+1 \right)^{1/2} \left(E_j + E_{j''} - \hbar\omega \right)\,, \end{aligned} \tag{8}$$

where

$$\begin{aligned} \beta_{jj'} &= \left\langle j \left\| Y^{(2)} \right\| j' \right\rangle \left(u_j v_{j'} + v_j u_{j'} \right)\,, \\ u_j^2 &= 1 - v_j^2\,. \end{aligned} \tag{9}$$

The occupation probabilities for the single-particle orbitals j are denoted with v_j^2, while A_0, Λ_0, and Γ_0 are free parameters.

The IBFM-1 calculations were conducted using the program package ODDA [60]. An initial set of single-particle energies and interaction parameters was adopted from Ref. [34]. These values were further varied to better reproduce the experimental data for ^{115}Ag.

BCS calculations were performed to determine the occupation probabilities and quasiparticle energies of the orbitals in ^{115}Ag. A value of $\Delta = 1.5$ MeV was considered for the pairing gap in the calculations. Results of the BCS procedure are shown in Table 3.

Table 3. BCS calculated occupation probabilities v_j^2 and quasiparticle energies E_j of the proton single-particle orbitals with energies ε_j in ^{115}Ag.

	ε_j [MeV]	v_j^2	E_j
$p_{3/2}$	0.0	0.95	3.40
$f_{5/2}$	0.4	0.94	3.05
$p_{1/2}$	2.6	0.64	1.57
$g_{9/2}$	2.1	0.77	1.78
$d_{5/2}$	5.0	0.10	2.46

Both the positive- and negative-parity states in ^{115}Ag were calculated by using the same boson–fermion interaction parameters. Values of $A_0 = -0.48$ MeV, $\Gamma_0 = 0.38$ MeV, and $\Lambda_0 = 3.5$ MeV^2 were considered, leading to the level schemes presented in Fig. 2.

Reduced M1 and E2 probabilities for transitions in ^{115}Ag were also calculated within IBFM-1. Operators in the following forms were used:

$$T(\mathrm{M1}) = \sqrt{\frac{90}{4\pi}} g_d \left(d^\dagger \tilde{d}\right)^{(1)} - g_F \sum_{jj'} \left(u_j u_{j'} + v_j v_{j'}\right) \langle j \| g_l l + g_s s \| j' \rangle \left[\left(a_j^\dagger \tilde{a}_{j'}\right)^{(1)} + \mathrm{c.c.}\right], \tag{10}$$

$$T(\mathrm{E2}) = e_B \left(\left(s^\dagger \tilde{d} + d^\dagger s\right)^{(2)} + \chi \left(d^\dagger \tilde{d}\right)^{(2)}\right) - e_F \sum_{jj'} \left(u_j u_{j'} - v_j v_{j'}\right) \langle j \| Y^{(2)} \| j' \rangle \left[\left(a_j^\dagger \tilde{a}_{j'}\right)^{(2)} + \mathrm{c.c.}\right]. \tag{11}$$

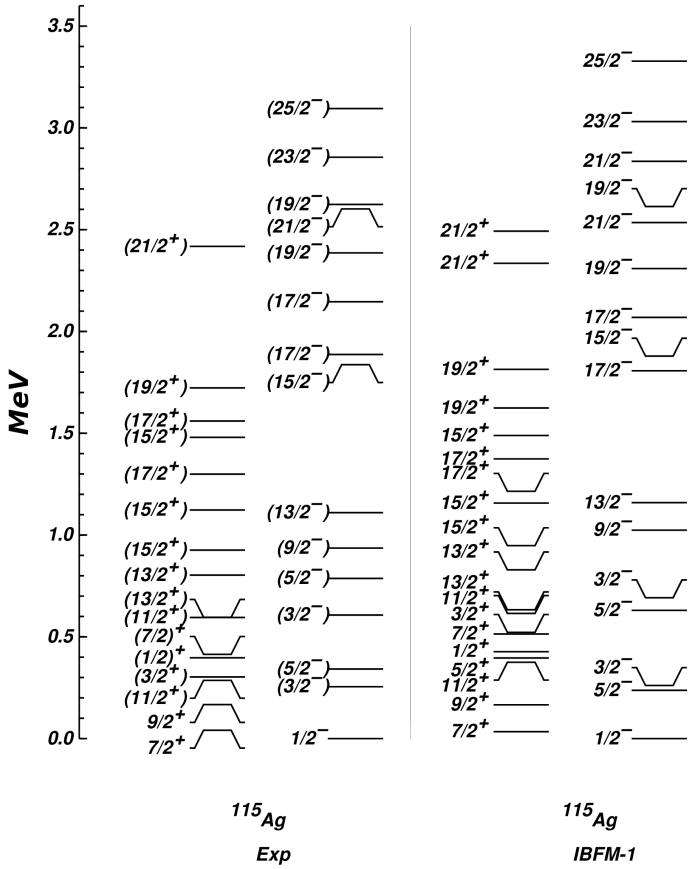

Fig. 2. IBFM-1 and experimental level energies in ^{115}Ag. The states with different parity are presented in separate sequences for visual convenience. The experimental data are taken from Ref. [61].

The effective boson and fermion charges (e_B and e_F, respectively) were set to be equal to the effective boson charge used in the ^{116}Cd IBM-1 calculations. The d-boson g-factor was set to $g_d = 0.3\ \mu_N$ based on the magnetic moment of the 2^+ state in the neighboring ^{116}Cd, and values of $g_s = 4.0\ \mu_N$ and $g_l = 1.0$ were applied.

B(M1) and B(E2) rates were calculated for some of the low-lying excited states in ^{115}Ag and are listed in Table 4.

In addition, the information about electromagnetic properties was extended by calculating the magnetic dipole and electric quadrupole moments of several low-lying levels in ^{115}Ag. Results are presented in Table 5. The electromagnetic moments of the $7/2^+_1$ state calculated within IBFM-1 agree well with recently published experimental data [62].

Table 4. IBFM-1 transition probabilities for several transitions in ^{115}Ag.

J_i^π	$E^\dagger_{level}$ [keV]	J_f^π	$E^\dagger_{level}$ [keV]	E_γ [keV]	$B(M1)_{th}$ [W.u.]	$B(E2)_{th}$ [W.u.]
$9/2^+$	166.56	$7/2^+$	41.16	125.40	0.004	59
$11/2^+$	285.5	$9/2^+$	166.56	118.94	0.048	78
$11/2^+$		$7/2^+$	41.16	244.34		6.1
$13/2^+$	596.7	$11/2^+$	285.5	311.20	0.187	72
$13/2^+$		$9/2^+$	166.56	430.14		19
$15/2^+$	926.8	$13/2^+$	596.7	330.10	0.241	60
$15/2^+$		$11/2^+$	285.5	641.30		32

Table 5. Magnetic dipole and electric quadrupole moments of low-lying states in ^{115}Ag calculated within IBFM-1. The experimental data for the electromagnetic moments of the $7/2^+$ state are taken from Ref. [62].

J^π	$E^\dagger_{level}$ [keV]	$\mu^\ddagger_{exp}$ [μ_N]	μ_{th} [μ_N]	$Q^\ddagger_{exp}$ [b]	Q_{th} [eb]
$1/2^-$	0.0		0.013		
$7/2^+$	41.16	4.4223 (9)	4.188	1.04 (8)	1.298
$9/2^+$	166.56		5.092		0.766
$(3/2^-)$	255.48		0.813		−0.414
$(5/2^-)$	342.62		0.515		−0.561

†from [61]
‡from [62]

3. Discussion

The IBFM-1 model provides a satisfactory description of the complex structure of ^{115}Ag, even though it assumes a single-fermion–boson coupling and no distinction between protons and neutrons is being made.

To better understand the theoretical results, the structure of the wave functions of the lowest-lying states in ^{115}Ag was studied. The IBFM-1 calculated contributions of different single-particle orbitals to the first three IBFM-1 levels are presented in Table 6.

The calculations show that the $\pi g_{9/2}$ orbit dominates the structure at low energies. Within the model, the role of the $\pi g_{9/2}^{-3}$ configuration is effectively taken into account by the interaction between the $\pi g_{9/2}^{-2}$ d boson and the $\pi g_{9/2}$ fermion.

Table 6. Single-particle contributions to the wave functions of some of the lowest-energy states in ^{115}Ag, as calculated in the present work.

J^π	$E^\dagger_{\text{level}}$ [keV]	$\pi p_{3/2}$ [%]	$\pi f_{5/2}$ [%]	$\pi p_{1/2}$ [%]	$\pi g_{9/2}$ [%]	$\pi d_{5/2}$ [%]
$1/2^-$	0.0	7.25	13.61	79.14	0.0	0.0
$7/2^+$	41.16	0.0	0.0	0.0	97.29	2.71
$9/2^+$	166.56	0.0	0.0	0.0	95.18	4.82

†from [61]

The $j-1$ anomaly, which is generally challenging to reproduce, is well described in the present work. A major part of this agreement with experimental data is due to the selected boson–fermion interaction parameter values. In line with observations from the IBFM calculations of lower-mass Ag nuclei [46, 47], it was found that the proper ordering of levels can be obtained through the exchange term in the particle–core coupling. Furthermore, the model not only reproduces the anomaly in the sequence of the $9/2^+$ and $7/2^+$ states, but it also predicts an enhanced E2 component of the $9/2^+ \rightarrow 7/2^+$ transition, as well as a hindered M1 component. This agrees with the observed probabilities for the same M1+E2 transition in lighter Ag isotopes [29].

The B(M1) and B(E2) values shown in Table 4 point to a similar structure of higher-spin yrast states in ^{115}Ag. The transition probabilities indicate strong E2 components and suggest that the levels are strongly correlated with the even–even core excitations.

The experimental energies of negative-parity states in ^{115}Ag are also well described by the model. The calculations show that the structure of the lowest-lying negative-parity levels is mainly dominated by the $\pi p_{1/2}$ orbital.

Although the experimental information about the electromagnetic properties of ^{115}Ag is sparse, recent measurements provide important data about the magnetic dipole and electric quadrupole moments of the $7/2^+_1$ state in this nucleus. Reference [62] presents a systematic study of these observables along part of the Ag isotopic chain. The results in the mid-shell silver nuclei are consistent and agree well with the theoretical values in the present work and Ref. [34]. This further validates the described IBFM-1 algebraic approach to the structure of ^{115}Ag.

Within the model concepts, the present calculations suggest a proton hole coupling to a core which generally exhibits many of the U(5) features but the calculations suggest a departure from the exact symmetry. Still, additional experimental data, especially for probabilities of electromagnetic

transitions and static electromagnetic moments, are essential to build a more coherent understanding of the characteristics of this isotope, as well as other mid-shell odd-A silver nuclei.

4. Conclusion

The structure of ^{115}Ag was studied within the IBFM-1 theoretical model. An odd-proton hole was coupled to an IBM-1 ^{116}Cd core and calculations were performed using five single-particle orbitals. The $j-1$ anomaly effect in ^{115}Ag was reproduced and the theoretical energies of low-lying states agree well with the experimental data. Even though it is difficult to draw firm conclusions due to a lack of precise experimental data, the new calculations indicate that a significant degree of collectivity is involved in the $9/2^+_1 \rightarrow 7/2^+_1$ transition. The model calculations suggest that collectivity persists at higher energies and spins but further experimental data are needed to test this hypothesis. The theoretical results outline the major role of the $\pi g_{9/2}$ orbital which dominates the structure of the low-lying positive-parity states in ^{115}Ag.

This work was funded by the Bulgarian National Science Fund under contract number KP-06-N68/8 and the European Union — Next Generation EU, the National Recovery and Resilience Plan of the Republic of Bulgaria, project No. BG-RRP-2.004-0008-C01. S.K. is supported by the Director, Office of Science, Office of High Energy Physics of the U.S Department of Energy under contract No. DE-AC02-05CH11231. The authors are grateful to Piet Van Isacker for the constructive discussions regarding the IBFM calculations.

REFERENCES

[1] J. Sharpey-Schafer, J. Simpson, «Escape suppressed spectrometer arrays: A revolution in γ-ray spectroscopy», *Prog. Part. Nucl. Phys.* **21**, 293 (1988).

[2] I. Lee, «The GAMMASPHERE», *Nucl. Phys. A* **520**, C641 (1990).

[3] I.Y. Lee, M.A. Deleplanque, K. Vetter, «Developments in large gamma-ray detector arrays», *Rep. Prog. Phys.* **66**, 1095 (2003).

[4] S. Akkuyun *et al.*, «AGATA — Advanced GAmma Tracking Array», *Nucl. Instrum. Methods Phys. Res. A* **668**, 26 (2012).

[5] H. Penttilä *et al.*, «First observation of the beta decay of ^{117}Pd and the discovery of a new isotope ^{119}Pd», *Z. Phys. A* **338**, 291 (1991).

[6] H. Geissel, «The GSI projectile fragment separator (FRS): a versatile magnetic system for relativistic heavy ions», *Nucl. Instrum. Methods Phys. Res. B* **70**, 286 (1992).

[7] I. Ahmad, W.R. Phillips, «Gamma rays from fission fragments», *Rep. Prog. Phys.* **58**, 1415 (1995).

[8] V.N. Fedoseyev *et al.*, «Study of short-lived silver isotopes with a laser ion source», *Z. Phys. A* **353**, 9 (1995).

[9] N. Hoteling *et al.*, «Onset of isomers in ^{125,126,127,128}Cd and weakened neutron–neutron interaction strength», *Phys. Rev. C* **76**, 044324 (2007).

[10] S. Ansari *et al.*, «Experimental study of the lifetime and phase transition in neutron-rich ^{98,100,102}Zr», *Phys. Rev. C* **96**, 054323 (2017).

[11] F. Browne *et al.*, «Lifetime measurements of the first states in ^{104,106}Zr: Evolution of ground-state deformations», *Phys. Lett. B* **750**, 448 (2015).

[12] Ł.W. Iskra *et al.*, «Revised B(E3) transition rate and structure of the 3^- level in ^{96}Zr», *Phys. Lett. B* **788**, 396 (2019).

[13] S. Lalkovski *et al.*, «Octupole collectivity in ^{98,100,102}Mo», *Phys. Rev. C* **75**, 014314 (2007).

[14] Y.X. Luo *et al.*, «New level schemes with high-spin states of ^{105,107,109}Tc», *Phys. Rev. C* **70**, 044310 (2004).

[15] A.M. Bruce *et al.*, «Shape coexistence and isomeric states in neutron-rich ^{112}Tc and ^{113}Tc», *Phys. Rev. C* **82**, 044312 (2010).

[16] S. Lalkovski *et al.*, «Coexisting structures in ^{105}Ru», *Phys. Rev. C* **89**, 064312 (2014).

[17] S. Kisyov *et al.*, «Structure of low-lying positive-parity states in ^{99,101,103}Ru from in-beam fast-timing measurements», *Bulg. J. Phys.* **42**, 583 (2015).

[18] S. Kisyov *et al.*, «Triaxial isomer in ^{103}Ru», *Bulg. J. Phys.* **43**, 195 (2016).

[19] S. Lalkovski *et al.*, «Submicrosecond isomer in $^{117}_{45}$Rh$_{72}$ and the role of triaxiality in its electromagnetic decay rate», *Phys. Rev. C* **88**, 024302 (2013).

[20] S. Lalkovski *et al.*, «Two-quasiparticle and collective excitations in transitional ^{108,110}Pd nuclei», *Eur. Phys. J. A* **18**, 589 (2003).

[21] E.A. Stefanova *et al.*, «Observation of positive-parity bands in ^{109}Pd and ^{111}Pd: Enhanced γ softness», *Phys. Rev. C* **86**, 044302 (2012).

[22] D. Ivanova *et al.*, «Structure of the low-lying states in ^{99,101,103,105}Pd», *Phys. Rev. C* **105**, 034337 (2022).

[23] E.R. Gamba *et al.*, «Fast-timing measurements in the ground-state band of ^{114}Pd», *Phys. Rev. C* **100**, 044309 (2019).

[24] W. Greiner, J.A. Maruhn, «Nuclear Models», *Springer*, 1995.

[25] R.F. Casten, «Nuclear Structure from a Simple Perspective», *Oxford Science Publ.*, New York 2000.

[26] S. Lalkovski, S. Kisyov, «Evolution of the $j-1$ anomalous states of the j^{-3} multiplets», *Phys. Rev. C* **106**, 064319 (2022).

[27] A. de-Shalit, I. Talmi, «Nuclear Shell Theory», *Academic Press*, New York, London 1963.

[28] V. Paar, «Coupling of a three-particle (hole) valence-shell cluster to quadrupole vibrations (Alaga model): The $Z = 50$ region: odd Ag and I isotopes; and the $Z = 28$ region: odd Mn and Ga isotopes», *Nucl. Phys. A* **211**, 29 (1973).

[29] National Nuclear Data Center (NNDC) database, https://www.nndc.bnl.gov/

[30] B.H. Flowers, «Studies in jj-Coupling. IV. The $g_{9/2}$-Shell», *Proc. R. Soc. Lond. A* **215**, 398 (1952).

[31] L.S. Kisslinger, «A note on coupling schemes in odd-mass nuclei», *Nucl. Phys.* **78**, 341 (1966).

[32] A. Escuderos, L. Zamick, «Seniority conservation and seniority violation in the $g_{9/2}$ shell», *Phys. Rev. C* **73**, 044302 (2006).

[33] P. Van Isacker, S. Heinze, «Seniority in quantum many-body systems. I. Identical particles in a single shell», *Ann. Phys.* **349**, 73 (2014).

[34] S. Lalkovski *et al.*, «Structure of the neutron mid-shell nuclei ^{111,113}Ag$_{64,66}$», *Phys. Rev. C* **96**, 044328 (2017).

[35] L. Zamick, «The nuclear $g_{9/2}$ shell — Comparison of our work with an old B.H. Flowers paper», arXiv:2210.01569 [nucl-th].

[36] S. Lalkovski *et al.*, «Core-coupled states and split proton–neutron quasiparticle multiplets in $^{122-126}$Ag», *Phys. Rev. C* **87**, 034308 (2013).

[37] S. Lalkovski, «$j - 1$ Anomaly through the Silver Isotopic Chain», *Bulg. J. Phys.* **44**, 498 (2017).

[38] S. Lalkovski, S. Kisyov, O. Yordanov, «$j - 1$ anomalous states and electromagnetic transition rates in the neutron mid-shell Ag nuclei», *Acta Phys. Pol. B* **55**, 1-A2 (2024).

[39] A. De-Shalit, «Core Excitations in Nondeformed, Odd-A, Nuclei», *Phys. Rev.* **122**, 1530 (1961).

[40] S. Nilsson, I. Ragnarsson, «Shapes and Shells in Nuclear Structure», *Cambridge University Press*, 1995.

[41] F. Iachello, O. Scholten, «New coupling scheme in the interacting boson–fermion model: O(6) spectra in odd-A nuclei», *Phys. Lett. B* **91**, 189 (1980).

[42] R.A. Ward, H. Beer, «On the Origin of the Solar-system Abundances of ^{113}In, ^{114}Sn, ^{115}Sn», *Astron. Astrophys.* **103**, 189 (1981).

[43] Zs. Nemeth *et al.*, «Nucleosynthesis in the Cd–In–Sn Region», *Astrophys. J.* **426**, 357 (1994).

[44] F. Iachello, P. Van Isacker, «The Interacting Boson–Fermion Model», *Cambridge University Press*, 1991.

[45] J. Rogowski *et al.*, «Intruder states in odd-A Ag isotopes», *Phys. Rev. C* **42**, 2733 (1990).

[46] U. Kaup *et al.*, «A Test of the interactig boson fermion model and its microscopical basis in transitional Tc and Ag nuclei», *Phys. Lett. B* **106**, 439 (1981).

[47] P. von Brentano, A. Gelberg, U. Kaup, «Description of Odd Mass Nuclei in the Interacting Boson-Fermion Model», in: F. Iachello (Ed.) «Interacting Bose–Fermi Systems in Nuclei», *Plenum*, New York 1981.

[48] L.D. Wood *et al.*, «Gyromagnetic ratios of excited states in ^{107,109}Ag», *Nucl. Phys.* **427**, 639 (1984).

[49] G. Maino, A. Mengoni, «One-nucleon-transfer reactions for Ag isotopes in the interacting boson–fermion model», *Phys. Rev. C* **38**, 2520 (1988).

[50] E. Galindo *et al.*, «Lifetime measurements of high-spin states in ^{101}Ag and their interpretation in the interacting boson fermion plus broken pair model», *Phys. Rev. C* **64**, 034304 (2001).

[51] P.O. Lipas, P. Toivonen, D.D. Warner, «IBA consistent-Q formalism extended to the vibrational region», *Phys. Lett. B* **155**, 295 (1985).

[52] D. Bucurescu *et al.*, «An extended IBA consistent-Q formalism applied to Ru and Pd isotopes», *Z. Phys. A* **324**, 387 (1986).

[53] O. Scholten, «The program package PHINT», KVI internal report KVI-63, Kernfysisch Versneller Instituut Groningen, 1979.

[54] S. Kisyov, D. Bucurescu, J. Jolie, S. Lalkovski, «Algebraic approach to the structure of the low-lying states in $A \approx 100$ Ru isotopes», *Phys. Rev. C* **93**, 044308 (2016).

[55] J. Blachot, «Nuclear Data Sheets for $A = 116$», *Nucl. Data Sheets* **111**, 717 (2010).

[56] J. Stachel, P. Van Isacker, K. Heyde, «Interpretation of the $A \approx 100$ transitional region in the framework of the interacting boson model», *Phys. Rev. C* **25**, 650 (1982).

[57] F. Iachello, O. Scholten, «Interacting Boson–Fermion Model of Collective States in Odd-A Nuclei», *Phys. Rev. Lett.* **43**, 679 (1979).

[58] J. Jolie *et al.*, «Multilevel description of the Rh isotopes in the interacting boson–fermion model», *Nucl. Phys. A* **438**, 15 (1985).

[59] O. Scholten, «The Interacting Boson Model Approximation», Ph.D. Thesis, University of Groningen, Groningen, 1980.

[60] O. Scholten, «The program package ODDA», KVI internal report no.255, Kernfysisch Versneller Instituut, Groningen, 1980.

[61] J. Blachot, «Nuclear Data Sheets for $A = 115$», *Nucl. Data Sheets* **113**, 2391 (2012).

[62] R.P. de Groote *et al.*, «Measurements of binding energies and electromagnetic moments of silver isotopes — A complementary benchmark of density functional theory», *Phys. Lett. B* **848**, 138352 (2024).